Applied Surface Science 357 (2015) 696–703

Contents lists available at ScienceDirect

Applied Surface Science

journal homepage: www.elsevier.com/locate/apsusc

# The performance of supercapacitor electrodes developed from chemically activated carbon produced from waste tea

I. Isil Gurten Inal[a,b], Stuart M. Holmes[b], Anthony Banford[b], Zeki Aktas[a,*]

[a] Department of Chemical Engineering, Faculty of Engineering, Ankara University, Tandogan 06100, Ankara, Turkey
[b] School of Chemical Engineering and Analytical Sciences, The University of Manchester, Sackville Street, Manchester M13 9PL, UK

ARTICLE INFO

*Article history:*
Received 23 June 2015
Received in revised form 2 September 2015
Accepted 6 September 2015
Available online 8 September 2015

*Keywords:*
Activated carbon
Supercapacitor
Waste tea
Chemical activation
Pore size characterisation

ABSTRACT

Highly microporous and mesoporous activated carbons were produced from waste tea for application as supercapacitor electrodes, utilising a chemical activation method involving treatment with either $K_2CO_3$ or $H_3PO_4$. The area, pore structure characteristics and surface functionality of the activated carbons were evaluated to investigate the influence on electrochemical performance. The performance of the activated carbons as supercapacitor electrodes was tested by cyclic voltammetry (CV), impedance spectroscopy (EIS) and galvanostatic charge–discharge (GCD) measurements, in an aqueous electrolyte. The results showed that the pore structure and type of the activated carbon have significant impact on the supercapacitor performance. Both waste tea-based activated carbon electrodes showed good cyclic stability. However, despite its lower specific surface area the highly microporous activated carbon produced with $K_2CO_3$, exhibited much better capacitive performance than that of the mesoporous activated carbon produced with $H_3PO_4$.



## 1. Introduction

Supercapacitors, also known as electric double layer capacitors (EDLC), represent an increasingly important class of electrical energy storage devices, which have received much international attention recently [1]. Supercapacitors fill the range between conventional dielectric capacitors and primary or secondary batteries in terms of their specific power and specific energy. Due to their highly reversible charge storage process, supercapacitors have longer cycle-lives and can be both rapidly charged and discharged at power densities exceeding 1 kW $kg^{-1}$ [2].

Supercapacitors have become attractive for use in high power devices due to their good power and energy densities, short charging times, long life cycle, and environmentally less harmful features. They are especially exciting for applications which require energy in bursts over short period of time such as telecommunications equipment, back-up power systems, and various electric/hybrid vehicles [3–6].

Porous carbon materials are widely used as electrode materials because of their high surface area. Activated carbons produced from natural materials such as different biomasses are an attractive and economic option for use as electrode materials. Activated carbon represents about half the total material cost of a supercapacitor, the low cost of biomass derived activated carbon electrodes, is a formidable barrier to entry for other carbons [7]. Over recent years a considerable amount of literature has been published on the usage of biomass based porous materials as electrode materials [8–12].

For this application, an activated carbon electrode with high capacitance is ideal; this requires the carbon to have not only a high surface area but also an optimised pore size distribution. The porosity of activated carbon can be tailored to the desired pore size distribution by varying the activation process or the type of precursor [13].

There are two processes for the preparation of activated carbon: physical and chemical activation. Physical activation involves carbonisation of a carbonaceous material followed by activation of the resulting char in the presence of activating agents such as $CO_2$ or steam. In chemical activation, the raw material is impregnated with activating agents such as $H_3PO_4$, KOH, $K_2CO_3$ or $ZnCl_2$ and then the impregnated material is heat-treated in an inert atmosphere at various temperatures [14,15]. The behaviour of the different agents during chemical activation influences the nature and characteristics of the final product. While in the use of $K_2CO_3$, KOH, and $ZnCl_2$ the activated carbons had large surface areas and greater micropore structure [16–19], in the use of $H_3PO_4$ as a chemical activating agent, the pore size distributions were more heterogeneous for the activated carbons obtained from olive and peach stones as precursors [20].

* Corresponding author.

http://dx.doi.org/10.1016/j.apsusc.2015.09.067
0169-4332/

Activated carbons prepared by physical or chemical activation methods usually have a wide pore size distribution from ultramicropores (<0.7 nm), and -micropores (<2 nm) to mesopores (2–50 nm) and macropores (>50 nm). Only the surface of the pores that the ions can access contribute to double layer capacitance, therefore the pore size must be large enough [21]. For aqueous EDLCs, since the size of a single nitrogen molecule is similar to that of hydrated $OH^-$ or $K^+$, those micropores that can adsorb nitrogen molecules at 77 K are also generally available for the electro adsorption of simple hydrated ions [1,22]. Recently, a number of studies have found that microporous carbons with pore sizes ranging from 0.7 to 2 nm show a high capacitive performance [23,24]. Moreover, some studies have reported that the maximum double layer capacitance is obtained with a pore size distribution which is very close to the electrolyte ion size. Both larger and smaller pores lead to a significant drop in capacitance [25]. However several studies reported that mesoporous carbons showed high capacitive performance compared with microporous carbons [26,27]. There is a discrepancy in existing literature regarding the effect of pore sizes on the capacitive performance [23,24,28,29]. In addition to surface area and pore size distribution, electrochemical performance depends on the wettability of porous carbons by the electrolyte which is determined by surface chemistry.

In the present study two activated carbon samples with different pore size distributions and surface functionalities were produced from the waste tea using $K_2CO_3$ and $H_3PO_4$ as activation agents. The reagents were chosen to prepare activated carbon with different pore sizes and surface structures. Activation with $K_2CO_3$ required a high temperature (800 °C) for the heating process, however, the temperature was lower (450 °C) for activation in the presence of $H_3PO_4$. The activated carbon samples were used as electrode materials in supercapacitors. The main objectives of the study were to evaluate the performance of the electrodes and to determine the effects of the activation agents ($K_2CO_3$ and $H_3PO_4$) on the surface properties of the activated carbon and on their supercapacitive performance in an aqueous electrolyte.

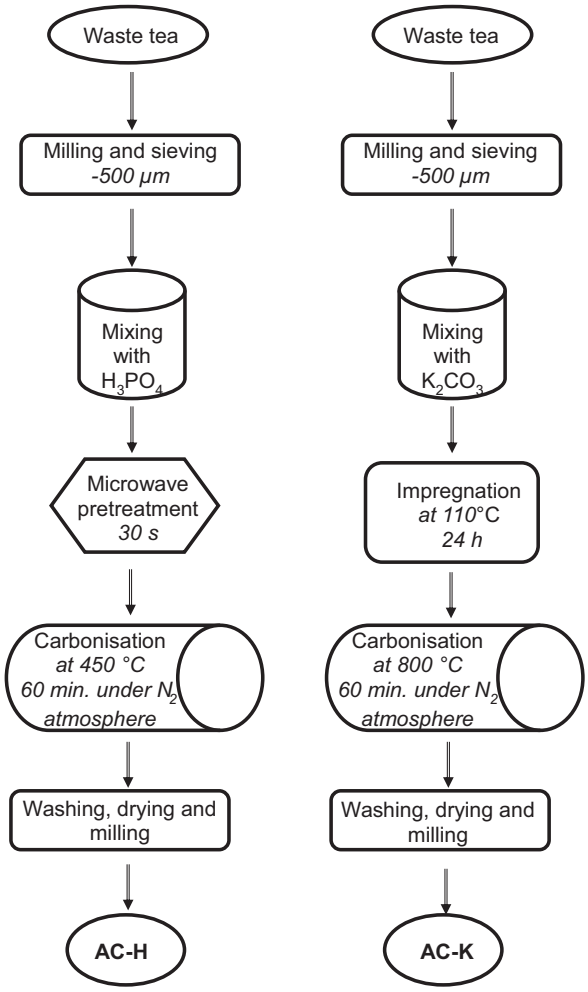


**Fig. 1.** The schematic illustration of the production processes of the activated carbon samples.

## 2. Materials and methods

### 2.1. Materials

The waste tea (WT) was collected from a tea factory in the Eastern Black Sea region of Turkey. Prior to the experiments, the raw material was crushed and sieved. Samples under 500 μm size were used. Two different chemically activated carbons were prepared from the waste tea. An 85% (wt) $H_3PO_4$ (Merck) solution and anhydrous $K_2CO_3$ (Sigma Aldrich) were used as chemical activating agents.

### 2.2. Production of activated carbons

The $H_3PO_4$ impregnated precursor was directly subjected to microwave (MW) pretreatment, whereas the $K_2CO_3$ activated carbon was prepared by conventional heating. Details of the production procedures were reported in previous articles [30–33]. Production conditions of the activated carbon samples such as impregnation ratio, carbonisation temperature which produced the highest BET specific surface area value for both chemical activation agents were chosen from the literature [30,31], and a schematic illustration of the production processes is given in Fig. 1.

The samples which were prepared with $H_3PO_4$ and $K_2CO_3$ activation are subsequently referred as AC-H and AC-K, respectively.

### 2.3. Surface characterisation of activated carbon samples

Nitrogen adsorption–desorption isotherms of the samples were determined using a Quantachrome NOVA 2200 series volumetric gas adsorption instrument. The total surface areas of the samples were measured according to the BET method [34] using the nitrogen adsorption isotherm data (below $P/P_o = 0.35$). The pore volume of each sample was determined in accordance with the Non-Local Density Functional Theory (NLDFT) method using the slit/cylindrical pore model. The micropore volume was determined by interpolation using the NLDFT pore size distribution data at 2 nm. In order to determine the mesopore volume, the micropore volume at 2 nm was subtracted from the total pore volume.

The surface features of the carbon samples were characterised by a FEI Quanta 200 scanning electron microscope (SEM). Prior to the examination of the samples, the solid particles were coated with thin layer of gold.

The surface functional groups of the samples were detected by a Mattson 1000 FTIR (Fourier Transform Infrared Spectroscopy) spectrometer. The spectra were obtained in the range of 400–4000 $cm^{-1}$. Due to the high absorbance of the activated carbon samples, very thin KBr pellets were prepared with the mass ratio of 500:1 (KBr:AC). In order to show the degree of graphitisation of the activated carbons, Raman spectra of the samples were obtained at 633 nm with a Horiba Scientific LabRam Raman spectrometer. X-ray photoelectron spectroscopy (XPS) which was employed to

**Table 1**
Specific surface areas pore volumes and fractions of AC-H and AC-K.

| Sample | $S_{BET}$ ($m^2/g$) | $V_t$[a] ($cm^3/g$) | $V_{micro}$[b] ($cm^3/g$) | $V_{meso}$[c] ($cm^3/g$) | Microporosity (%) | Mesoporosity (%) |
|---|---|---|---|---|---|---|
| AC-H | 1327 | 1.142 | 0.2778 | 0.8651 | 24.31 | 75.69 |
| AC-K | 1125 | 0.592 | 0.5420 | 0.050 | 91.55 | 8.45 |

[a] At $P/P_o = 0.95$.
[b] At 2 nm.
[c] Total volume–micropore volume.

analyse the functional groups on the surface of AC-K and AC-H by a Thermo, K-Alpha monochromated high performance XPS.

### 2.4. Electrode preparation

Stainless steel plates (1 cm × 1 cm) were used as the current collectors. The surface of the stainless steel plates were etched using concentrated hydrochloric acid to create rougher surface for a better contact with the carbon sample.

The supercapacitor electrodes were prepared by mixing the activated carbon sample (85 wt.%), with polyvinylidene fluoride (PVdF) (5 wt.%, as binder) and carbon black (CB) (10 wt.%, as conductive additive), using N-methyl-2-pyrrolidone (NMP) as a solvent. The resultant slurry was sprayed on to the stainless steel plate. Then the electrodes were dried at 75 °C for 24 h under vacuum to remove the solvent. The mass of active material in a single electrode was around 1.5 mg. Both electrodes in one supercapacitor cell were identical. The electrodes were immersed into 1 M $H_2SO_4$ aqueous electrolyte solution until wetted. A commercial thin paper separator soaked in the electrolyte solution was used in order to prevent direct contact between the two electrodes. Finally, the symmetric supercapacitor device was assembled by sandwiching the paper separator between two identical electrodes.

### 2.5. Characterisation of electrodes

Cyclic voltammetry (CV), electrochemical impedance spectroscopy (EIS) and galvanostatic charge/discharge (GCD) techniques were employed to test the supercapacitive performance of electrodes. The tests were carried out with a two-electrode cell configuration under ambient conditions using an Autolab PGSTAT 3000 potentiostat/galvanostat. CV studies were performed in between 0 V and 0.8 V potential range at various scan rates (25, 50, 100, 150, 250 mV/s). The impedance plots were recorded using an amplitude of 5 mV rms in a frequency range from $10^4$ to 0.01 Hz at applied DC voltage of 0 V. GCD tests were carried out at 1.5, 2.5, 5, 7.5 mA/$cm^2$ constant current densities between 0 V and 0.8 V potential range. Stability tests of the electrodes were carried out by using the GCD technique at a constant current density of 1.5 mA/$cm^2$ at the same potential window. The specific capacitances of the electrodes were calculated by utilising galvanostatic charge/discharge curves at 1.5 mA/$cm^2$ of current density according to Eq. (1):

$$C_{spec} = \frac{2i\Delta t}{m\Delta V} \quad (1)$$

where, $C_{spec}$ (F/g) the specific capacitance; $i$ (A) is the current density; $\Delta t$ (s) is the change of the discharge process duration, $\Delta V$ (V) is the potential change during the discharge process and $m$ (g) is the mass of active material in one electrode.

Coulombic efficiencies (defined as the total charge removed divided by the total charge added to replenish the charge removed) were calculated using following equation:

$$\eta = \left(\frac{t_d}{t_c}\right) * 100 \quad (2)$$

where $t_d$ and $t_c$ are discharging and charging time of the electrodes, respectively [35].

## 3. Results and discussion

### 3.1. Characterisation of activated carbons

Nitrogen adsorption–desorption isotherms and the pore size distribution curves for AC-H and AC-K are presented in Fig. 2. The isotherms (Fig. 2a) of AC-H show the typical hysteresis loop with capillary condensation ($P/P_o > 0.45$). The hysteresis loop corresponds to type-IV isotherm according to the IUPAC classification, demonstrating its mesoporous structure. On the other hand, the shape of isotherm of AC-K is close to type-I, indicating the microporous character of the carbon material.

The pore size distribution curves (Fig. 2b) of the samples are significantly different. While AC-H has both micropores and mesopores, AC-K has a largely microporous structure. Table 1 provides key characteristic data from the isotherm and distribution curves for both samples. The total BET specific surface areas are 1327 and 1125 $m^2/g$ with the total pore volumes of 1.142, and 0.592 $cm^3/g$ for AC-H and AC-K, respectively. The micropore volumes of the AC-H and AC-K are 0.2778, and 0.5420 $cm^3/g$, corresponding to the micropore volume fractions of 24.31, and 91.55%, respectively. The substantial difference between the pore volumes (Table 1) and pore size distributions (Fig. 2b) of the carbon materials is due to different activation mechanisms of the chemical activation agents which are elucidated in previous works [22,23].

The surface morphologies of the activated carbon samples are shown in Fig. 3. The rough surface morphology can be observed on both samples. While AC-H has an irregular and grainy surface with different void sizes, AC-K has more regular crater like pores formed during the reactions between the waste tea and $K_2CO_3$. This type of pore may have been shaped during the release of reaction gases from the core of the particles towards the outer surface.

Fig. 4 presents the FTIR spectra of the activated carbon samples. As seen in the figure, both spectra show a wide absorption band at 3600–3300 $cm^{-1}$ with a maximum at around 3400 $cm^{-1}$. The

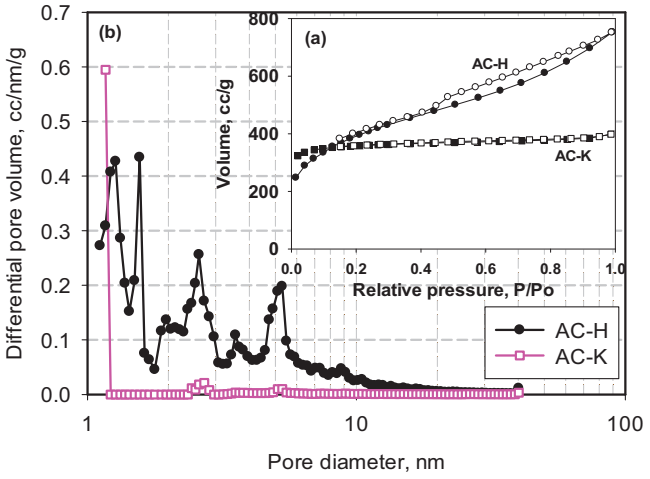


**Fig. 2.** Nitrogen adsorption–desorption isotherms (a) and pore size distribution curves (b) of the activated carbon samples.

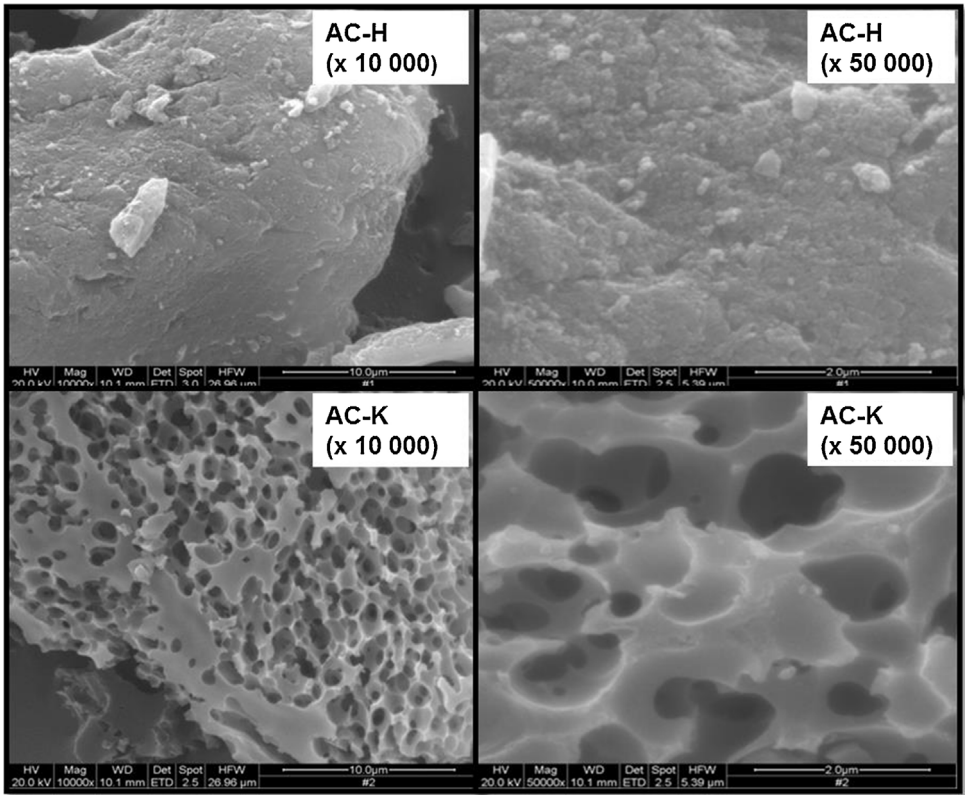


**Fig. 3.** SEM micrographs of the activated carbon samples.

position of the band is characteristic of the stretching vibration of hydroxyl compounds from phenols, alcohols and absorbed water while broadening of the band is indicative of a high degree of association because of extensive hydrogen bonding [36], this shows the hydrophilic character of the carbon samples, which is essential for the wettability of the electrodes with aqueous electrolyte [37]. The more intense hydroxyl band for AC-H can be assigned to the presence of a higher concentration of —OH groups, probably due to the milder production conditions. The adsorption bands in the 1500–1750 $cm^{-1}$ region are ascribed to C=O stretching vibrations of carboxylic acids and lactone groups and/or highly conjugated carbonyls (quinone groups) and C=C stretching vibrations in the aromatic ring. This band is very weak for the AC-K sample. It may be concluded that AC-K contains a less (or no) carboxylic groups. The broad bands at 1300–1000 $cm^{-1}$ have been assigned to the C—O stretching in acids, alcohols, phenols, ethers and esters. While these broad bands are distinctive for AC-H, the bands almost disappeared for the AC-K. This obviously indicates that C—O bonds in acids, alcohols, phenols, ethers and esters disappear during the high temperature carbonisation process of AC-K. Activation of the raw material with $K_2CO_3$ generates less functional groups compared with $H_3PO_4$ activation process due to the higher temperature of the $K_2CO_3$ process during carbonisation [11].

Raman spectra of the activated carbons are shown in Fig. 5. The Raman spectra of the activated carbons show two broad bands at

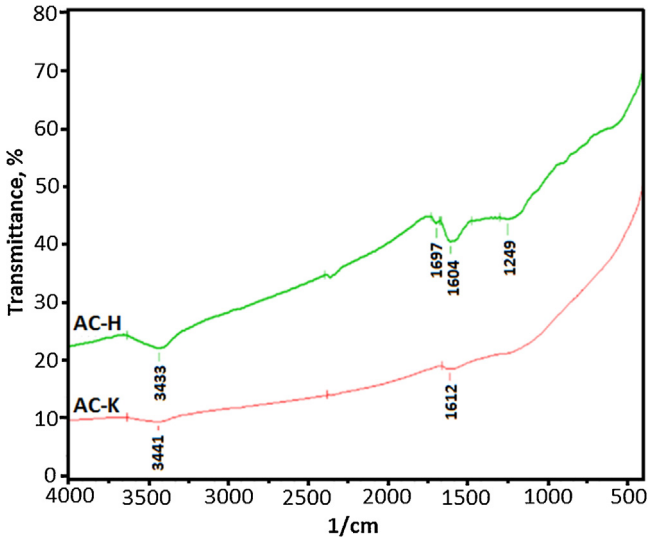


**Fig. 4.** FTIR spectra of the activated carbon samples.

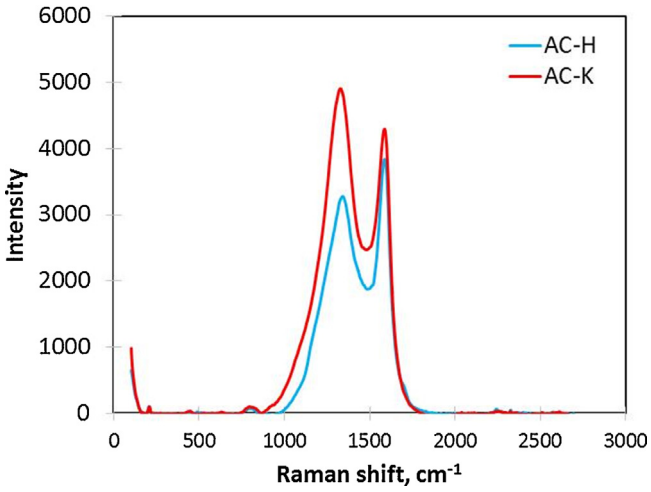


**Fig. 5.** Raman spectra of the activated carbon samples.

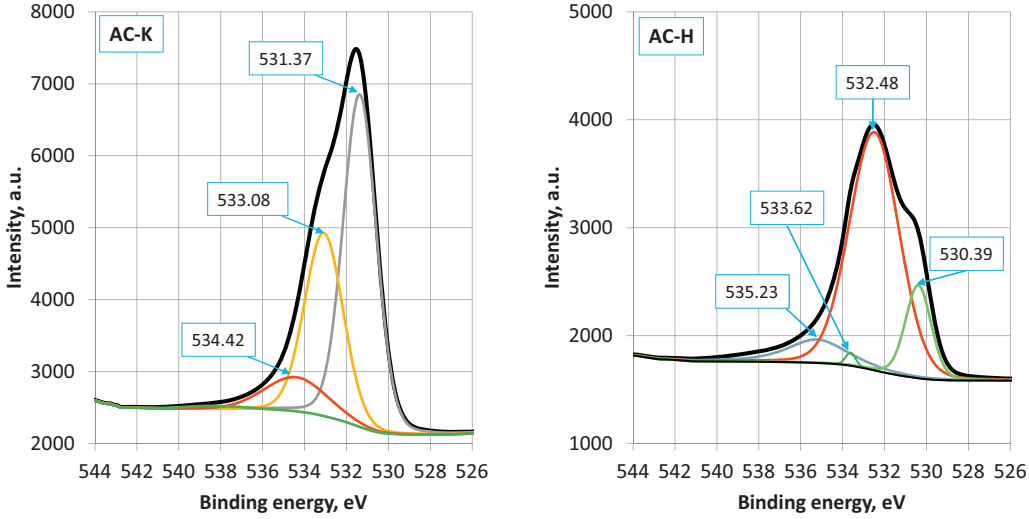


**Fig. 6.** XPS spectra (O 1s) of the activated carbon samples.

around 1580 $cm^{-1}$ (G band) and 1320 $cm^{-1}$ (D band), which correspond to the C—C bond vibrations of carbon atoms with $sp^2$ electronic configuration in graphene sheet structure and the disordered and imperfect structures of carbon materials, respectively. The graphitic degree of the carbonaceous materials is determined with the intensity ratio of D-band and G-band (ID/IG). An increase in the ratio indicates that the oxygen functional groups were removed and the graphene network ($sp^2$ carbon) was re-established during the activation process [38]. The ratios of ID/IG derived from the figure are $1.16 \pm 0.04$ for AC-K, $0.85 \pm 0.01$ for AC-H. This clearly indicated that AC-H has a relative higher graphitic degree, less disordered structure and higher oxygen functional groups than AC-K.

XPS O 1s spectra of the samples are shown in Fig. 6. The reports [39–41] in existing literature were considered to interpret the binding energy values of the O 1s orbital for the analyses. The O 1s spectra mainly display peaks of oxygen in carbonyl and carboxylic groups, oxygen in hydroxyl or ethers, chemisorbed oxygen and oxygen in water. The peak at 530.39 eV may belong to quinone, metal oxides [41,42]. The peaks at 531.4 eV and 532.48 eV probably show carboxylic (O=C—OH) and carbonyl groups (C=O). The peaks at 533.08 eV and 533.62 eV may confirm oxygen singly bonded to carbon in aromatic rings, in phenols and ethers. The peaks at 534.42 and 535.23 eV could correspond to chemisorbed oxygen in $H_2O$ and/or C—OH [39–41]. The O 1s spectra show that AC-K and AC-H have different functional groups (especially carboxylic groups), this may be attributed to their different electrode performances.

### 3.2. Electrochemical characterisation of electrodes

The most accurate specific capacitance ($C_{spec}$), the cyclic stability and reversibility of the electrode can be determined by using a galvanostatic charge–discharge technique [43]. The principle of this method is to investigate the time of current charge and discharge process performed by the measured electrode. A symmetrical triangle curve reflects ideal supercapacitive behaviour with good reversibility and high electrochemical stability [44]. Fig. 7a shows the galvanostatic charge–discharge curves of the AC-H and AC-K at a constant current density of 1.5 mA/$cm^2$. The charge–discharge curves of both electrodes are almost symmetrical, but the AC-H electrode has a small amount of internal resistance (IR) voltage drop, shown by a sudden potential drop at the very beginning of discharge process, leading to a higher contact resistant and slower

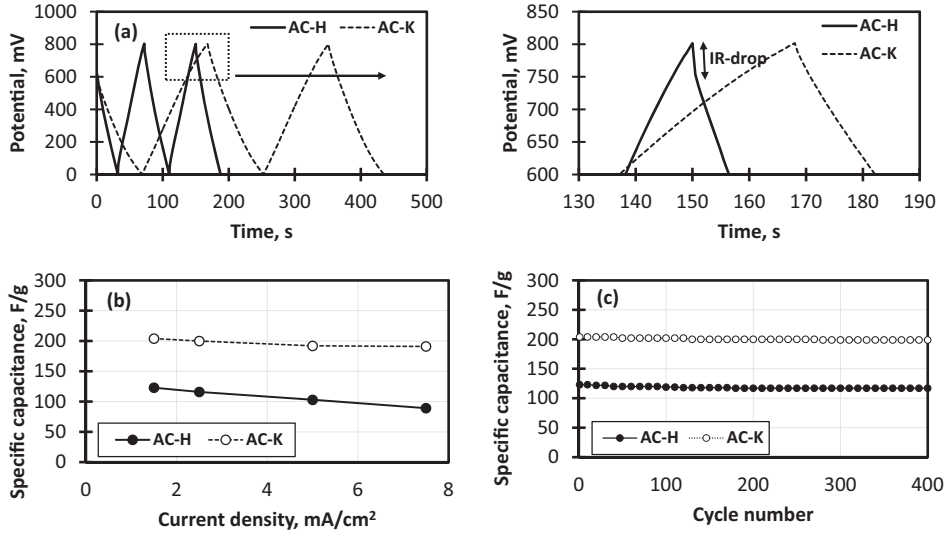


**Fig. 7.** (a) Galvanostatic charge–discharge curves of the electrodes at the current density of 1.5 mA/$cm^2$; (b) variation of specific capacitance of the electrodes versus current density; (c) cycling performance of the electrodes at the current density of 1.5 mA/$cm^2$.

**Table 2**
Charge–discharge characteristics of the supercapacitors.

| AC-H | | | AC-K | | |
|---|---|---|---|---|---|
| Cycle number | $C_{spec}$ (F/g) | Coulombic eff. (%) | Cycle number | $C_{spec}$ (F/g) | Coulombic eff. (%) |
| 1 | 123 | 89 | 1 | 203 | 96 |
| 200 | 118 | 88 | 200 | 200 | 95 |
| 400 | 117 | 86 | 400 | 199 | 94 |

ion transport rate than AC-K electrode. The charge–discharge time of the AC-K is also substantially longer than the charge–discharge time of the AC-H electrode. This proves that the AC-K can be charged with more electrolyte ions than the AC-H, indicating the higher specific capacitance and smaller resistance of the AC-K.

The specific capacitances of the electrodes were calculated using galvanostatic charge–discharge analysis data at various constant current densities. Fig. 7b exhibits the specific capacitance of the electrodes versus current density. The higher capacitance retention at high current density indicates a better supercapacitive performance of the electrode. This phenomenon can be explained by the decreasing accessibility of electrolyte ions into the active layer in the electrode matrix with increasing current density. This is due to the high polarisation of electrode and IR drop at high current density [45]. The highest specific capacitance of AC-K and AC-H electrodes are 203 F/g and 123 F/g at a current density of 1.5 mA/cm$^2$, respectively. While the capacitance of AC-K can still maintain 93% at the maximum current density of 7.5 mA/cm$^2$, the capacitance of AC-H is only 73% at the same current density. There is no study in the literature using waste tea as the raw material and $K_2CO_3$, $H_3PO_4$ as activating agents. However Peng et al. reported that the capacitance value was 330 F/g for the activated carbon produced from waste tea-leaves and KOH [46]. Various capacitance values such as 144 F/g [8], 243 F/g [9] and 124 F/g [47] were also reported using different activated carbons prepared from different starting materials.

The long term cycling performance of the electrodes as a function of the cycle numbers has been investigated for 400 cycles. The results are shown in Fig. 7c. There are no significant decreases in specific capacitance values after 400 cycles for both AC-H and AC-K. Whilst the AC-K electrode clearly shows better electrochemical performance, highly stable electrodes can be prepared from waste tea by both production methods.

Some charge–discharge characteristics of the supercapacitors are tabulated in Table 2. AC-K shows excellent cyclability (98%) and coulombic efficiency (94%) for the last cycle at a current density of 1.5 mA/cm$^2$. Also AC-H shows very good cyclic stability (95%) and coulombic efficiency (86%), indicating not quite significant ohmic drop in the discharge process.

Fig. 8a and b shows the CV curves of the AC-H and AC-K electrodes at different scan rates. It can be clearly observed that the current densities of AC-H electrodes are significantly lower than the current densities of AC-K electrode at all scan rates. All the CV curves of AC-K electrode exhibit quite a symmetric rectangular shapes even at high scan rates, implying a good charge propagation, quick ion diffusion within the pores, low contact resistance and fast re-organizing of the electrical double layer at the switching potentials [48,49]. On the other hand, the AC-H electrode shows excellent capacitive behaviour only at low scan rates, a distinct deviation from the rectangular shape is observed at 150 mV/s and 250 mV/s, which may be caused by the limitation in charge transfer processes due to the significant contribution of the equivalent series resistance. The considerable difference in electrochemical behaviour

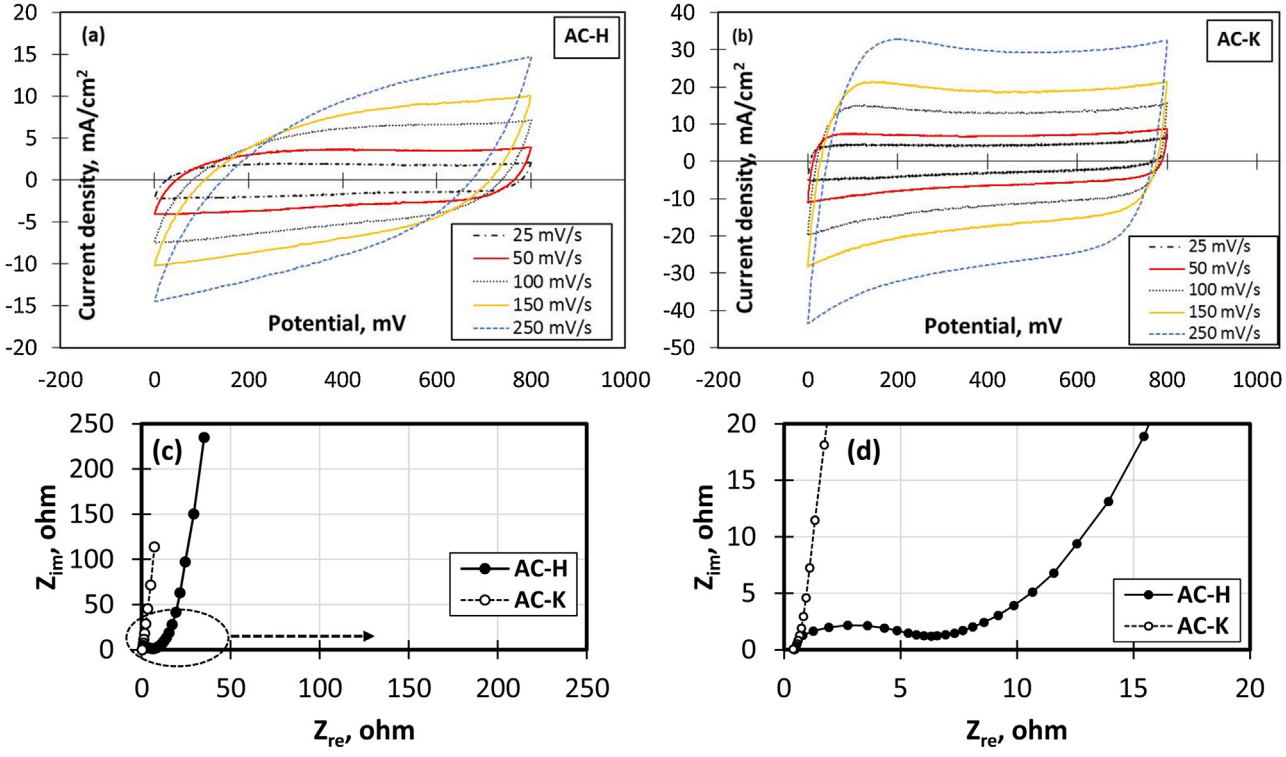


**Fig. 8.** (a) CV curves of the AC-H electrode; (b) CV curves of the AC-K electrode; (c) and (d) Nyquist plots of the electrodes.

between the two electrodes materials is related to their different porous structures and functionalities.

The electrochemical impedance spectroscopy (EIS) is used to describe the contact resistance, charge transfer resistance and the diffusion resistance in pores of electrolyte ions during the electrochemical process. In this technique, alternating current of low amplitude is applied at an open circuit potential to investigate the penetration ability of ions through the porous network of the electrode at different frequency [47]. Fig. 8c shows the impedance plots, known as the Nyquist curves, of the electrodes. The Nyquist plots of the electrodes show typical features of porous electrodes with a semicircle obtained at the high frequency region of the curves. The diameter of the semicircle is correlated with the resistance of the electrode itself and the contact resistance between electrode and current collector [8]. As seen in the figure, there is a small semicircle at high frequencies for the AC-K electrode, which indicates that the electrode exhibits quite a low internal resistance. The AC-H electrode has a dramatically larger semicircle than the AC-K electrode (Fig. 8d), implying it has higher internal resistance due to its heterogeneous porous structure and surface oxygen-containing functional groups [9,50]. This means that the pore accessibility of electrolyte ions throughout the AC-K electrode surface is more effective than the AC-H electrode. At low frequencies, the EIS spectrum of AC-K shows a line with a steeper slope which is rather different from that of AC-H, suggesting the ideal capacitance behaviour which may be owing to the its uniform microporous structure. The AC-K electrode, which has higher specific capacitance, shows lower internal contact resistance and diffusion resistance of the electrolyte ions in pores compared to AC-H. The EIS results are consistent with the results of CV and GCD measurements.

## 4. Conclusions

Highly reversible and stable supercapacitor electrodes were prepared from the waste tea based chemically activated carbons. The activated carbon derived from the waste tea by $K_2CO_3$ activation showed much better supercapacitive performance than that produced with $H_3PO_4$ activation in an aqueous electrolyte, despite having lower specific surface area. $K_2CO_3$ activation produced a more uniform microporous structure and less surface oxygen groups which resulted in a lower internal resistance and excellent electrochemical reversibility in aqueous electrolytes. Moreover, the surface area is not the only parameter that affects the capacitive performance; a well-developed microporous architecture plays a more significant role in the electrochemical performance, allowing the ions to move easily inside the porous structure.

## Acknowledgements

The authors gratefully acknowledge the support of the Scientific Research Projects Coordination Unit (BAP) of Ankara University, Turkey (Project No: 13B4343001) and I. Isil Gurten Inal gratefully acknowledges the support of this research through the International Doctoral Research Fellowship Programme of Scientific and Technological Research Council of Turkey (TUBITAK) and the University of Manchester (UK) for hosting the Fellowship. The authors are also grateful to Prof. Mustafa Gullu, Dr. Paul Coffey and Gamze Ulusoy for their assistance and suggestions on the paper.

## References

[1] E. Frackowiak, F. Béguin, Carbon materials for the electrochemical storage of energy in capacitors, Carbon 39 (6) (2001) 937–950.
[2] A. Shukla, Electrochemical power sources, Resonance 6 (8) (2001) 72–81.
[3] A. Pandolfo, A. Hollenkamp, Carbon properties and their role in supercapacitors, J. Power Source 157 (1) (2006) 11–27.
[4] I.M. De la Fuente Salas, Y.N. Sudhakar, M. Selvakumar, High performance of symmetrical supercapacitor based on multilayer films of graphene oxide/polypyrrole electrodes, Appl. Surf. Sci. 296 (2014) 195–203.
[5] W. Denga, W. Lana, Y. Suna, Q. Sua, E. Xie, Porous CoO nanostructures grown on three-dimension graphene foams for supercapacitors electrodes, Appl. Surf. Sci. 305 (2014) 433–438.
[6] D. Gui, C. Liu, F. Chen, J. Liu, Preparation of polyaniline/graphene oxide nanocomposite for the application of supercapacitor, Appl. Surf. Sci. 307 (2014) 172–177.
[7] L. Weinstein, R. Dash, Supercapacitor carbons, Mater. Today 16 (10) (2013) 356–357.
[8] M. Wu, P. Ai, M. Tan, B. Jiang, Y. Li, J. Zheng, W. Wu, Z. Li, Q. Zhang, X. He, Synthesis of starch-derived mesoporous carbon for electric double layer capacitor, Chem. Eng. J. 245 (2014) 166–172.
[9] X. He, P. Ling, M. Yu, X. Wang, X. Zhang, M. Zheng, Rice husk-derived porous carbons with high capacitance by $ZnCl_2$ activation for supercapacitors, Electrochim. Acta 105 (2013) 635–641.
[10] A. Elmouwahidi, Z. Zapata-Benabithe, F. Carrasco-Marín, C. Moreno-Castilla, Activated carbons from KOH-activation of argan (*Argania spinosa*) seed shells as supercapacitor electrodes, Bioresour. Technol. 111 (2012) 185–190.
[11] A. Ismanto, S. Wang, F. Soetaredjo, S. Ismadji, Preparation of capacitors electrode from cassava peel waste, Bioresour. Technol. 101 (10) (2010) 3534–3540.
[12] J. Xua, L. Chena, H. Qua, Y. Jiaoa, J. Xiea, G. Xing, Preparation and characterization of activated carbon from reedy grass leaves by chemical activation with $H_3PO_4$, Appl. Surf. Sci. 320 (2014) 674–680.
[13] E. Frackowiak, Q. Abbas, F. Béguin, Carbon/carbon supercapacitors, J. Energy Chem. 22 (2) (2013) 226–240.
[14] Y. Sudaryanto, S.B. Hartono, W. Irawaty, H. Hindarso, S. Ismadji, High surface area activated carbon prepared from cassava peel by chemical activation, Bioresour. Technol. 97 (5) (2006) 734–739.
[15] J. Hayashi, T. Horikawa, I. Takeda, K. Muroyama, F.N. Ani, Preparing activated carbon from various nutshells by chemical activation with $K_2CO_3$, Carbon 40 (13) (2002) 2381–2386.
[16] A. Mestre, E. Tyszko, M. Andrade, M. Galhetas, C. Freire, A. Carvalho, Sustainable activated carbons prepared from a sucrose-derived hydrochar: remarkable adsorbents for pharmaceutical compounds, RSC Adv. 5 (25) (2015) 19696–19707.
[17] A. El-Hendawy, An insight into the KOH activation mechanism through the production of microporous activated carbon for the removal of $Pb^{2+}$ cations, Appl. Surf. Sci. 255 (6) (2009) 3723–3730.
[18] P.T. Williams, A.R. Reed, Development of activated carbon pore structure via physical and chemical activation of biomass fibre waste, Biomass Bioenergy 30 (2) (2006) 144–152.
[19] F. Wu, R. Tseng, C. Hu, Comparisons of pore properties and adsorption performance of KOH-activated and steam-activated carbons, Microporous Mesoporous Mater. 80 (1–3) (2005) 95–106.
[20] M. Molina-Sabio, F. Rodriguez-Reinoso, Role of chemical activation in the development of carbon porosity, Colloids Surf. A 241 (1–3) (2004) 15–25.
[21] B. Xu, S. Hou, H. Duan, G. Cao, M. Chu, Y. Yang, Ultramicroporous carbon as electrode material for supercapacitors, J. Power Source 228 (2013) 193–197.
[22] H. Shi, Activated carbons and double layer capacitance, Electrochim. Acta 41 (10) (1996) 1633–1639.
[23] J. Chmiola, Anomalous increase in carbon capacitance at pore sizes less than 1 nanometer, Science 313 (5794) (2006) 1760–1763.
[24] J. Leis, M. Arulepp, A. Kuura, M. Lätt, E. Lust, Electrical double-layer characteristics of novel carbide-derived carbon materials, Carbon 44 (11) (2006) 2122–2129.
[25] C. Largeot, C. Portet, J. Chmiola, P. Taberna, Y. Gogotsi, P. Simon, Relation between the ion size and pore size for an electric double-layer capacitor, J. Am. Chem. Soc. 130 (9) (2008) 2730–2731.
[26] C. Arbizzani, S. Beninati, M. Lazzari, F. Soavi, M. Mastragostino, Electrode materials for ionic liquid-based supercapacitors, J. Power Source 174 (2007) 648–652.
[27] M. Lazzari, M. Mastragostino, F. Soavi, Capacitance response of carbons in solvent-free ionic liquid electrolytes, Electrochem. Commun. 9 (2007) 1567–1572.
[28] P.J. Hall, M. Mirzaeian, S.I. Fletcher, F.B. Sillars, A.J.R. Rennie, G.O. Shitta-Bey, G. Wilson, A. Cruden, R. Carter, Energy storage in electrochemical capacitors: designing functional materials to improve performance, Energy Environ. Sci. 3 (2010) 1238–1251.
[29] J.A. Fernaíndez, S. Tennison, O. Kozynchenko, F. Rubiera, F. Stoeckli, T.A. Centeno, Effect of mesoporosity on specific capacitance of carbons, Carbon 47 (2009) 1598–1604.
[30] I. Gurten, M. Ozmak, E. Yagmur, Z. Aktas, Preparation and characterisation of activated carbon from waste tea using $K_2CO_3$, Biomass Bioenergy 37 (2012) 73–81.
[31] E. Yagmur, M. Ozmak, Z. Aktas, A novel method for production of activated carbon from waste tea by chemical activation with microwave energy, Fuel 87 (15–16) (2008) 3278–3285.
[32] E. Yagmur, M.S. Tunc, A. Banford, Z. Aktas, Preparation of activated carbon from autohydrolysed mixed southern hardwood, J. Anal. Appl. Pyrolysis 104 (2013) 470–478.

[33] B. Tiryaki, E. Yagmur, A. Banford, Z. Aktas, Comparison of activated carbon produced from natural biomass and equivalent chemical compositions, J. Anal. Appl. Pyrolysis 105 (2014) 276–283.
[34] S. Brunauer, P.H. Emmett, E. Teller, Adsorption of gases in multimolecular layers, J. Am. Chem. Soc. 60 (1938) 309–319.
[35] V. Ganesh, S. Pitchumani, V. Lakshminarayanan, New symmetric and asymmetric supercapacitors based on high surface area porous nickel and activated carbon, J. Power Source 158 (2006) 1523–1532.
[36] A.M. Puziy, O.I. Poddubnaya, A. Martinez-Alonso, F. Suarez-Garcia, J.M.D. Tascon, Surface chemistry of phosphorus containing carbons of lignocellulosic origin, Carbon 43 (2005) 2857–2868.
[37] D.S. Yuan, J.H. Zeng, J.X. Chen, J.L. Liu, Highly ordered mesoporous carbon synthesized via in situ template for supercapacitors, Int. J. Electrochem. Sci. 4 (2009) 562–570.
[38] Z. Gao, N. Song, X. Li, Microstructural design of hybrid CoO@NiO and graphene nano-architectures for flexible high performance supercapacitors, J. Mater. Chem. A 3 (2015) 14833–14844.
[39] R. Arrigo, M. Havecker, S. Wrabetz, R. Blume, M. Lerch, J. McGregor, E.P.J. Parrott, J.A. Zeitler, L.F. Gladden, A. Knop-Gericke, R. Schlogl, D.S. Su, Tuning the acid/base properties of nanocarbons by functionalization via amination, J. Am. Chem. Soc. 132 (2010) 9616.
[40] C.M. Chen, Q. Zhang, X.C. Zhao, B. Zhang, Q.Q. Kong, M.G. Yang, Q.H. Yang, M.Z. Wang, Y.G. Yang, R. Schlogl, D.S. Su, Hierarchically aminated graphene honeycombs for electrochemical capacitive energy storage, J. Mater. Chem. 22 (2012) 14076.
[41] Y.J. Oh, J.J. Yoo, Y.I. Kim, J.K. Yoon, H.N. Yoon, J. Kim, S.B. Park, Oxygen functional groups and electrochemical capacitive behavior of incompletely reduced graphene oxides as a thin-film electrode of supercapacitor, Electrochim. Acta 116 (2014) 118–128.
[42] A.P. Terzyk, The influence of activated carbon surface chemical composition on the adsorption of acetaminophen (paracetamol) in vitro Part II. TG, FTIR, and XPS analysis of carbons and the temperature dependence of adsorption kinetics at the neutral pH, Colloids Surf. A 177 (2001) 23–45.
[43] D. Yiğit, T. Güngör, M. Güllü, Poly(thieno[3,4-b][1,4]dioxine) and poly([1,4]dioxino[2,3-c]pyrrole) derivatives: p- and n-dopable redox-active electrode materials for solid state supercapacitor applications, Org. Electron. 14 (12) (2013) 3249–3259.
[44] L. Yafei, H. Zhonghua, X. Kun, Z. Xiangwei, G. Qiang, Surface modification and performance of activated carbon electrode material, Acta Phys. Chim. Sin. 24 (2008) 1143–1148.
[45] C. Kim, S. Park, W. Lee, K. Yang, Characteristics of supercapacitor electrodes of PBI-based carbon nanofiber web prepared by electrospinning, Electrochim. Acta 50 (2–3) (2004) 877–881.
[46] C. Peng, X. Yan, R. Wang, J. Lang, Y. Ou, Q. Xue, Promising activated carbons derived from waste tea-leaves and their application in high performance supercapacitors electrodes, Electrochim. Acta 87 (2013) 401–408.
[47] D. Bhattacharjya, J. Yu, Activated carbon made from cow dung as electrode material for electrochemical double layer capacitor, J. Power Source 262 (2014) 224–231.
[48] D. Wu, X. Chen, S. Lu, Y. Liang, F. Xu, R. Fu, Study on synergistic effect of ordered mesoporous carbon and carbon aerogel during electrochemical charge–discharge process, Microporous Mesoporous Mater. 131 (1–3) (2010) 261–264.
[49] B. Fang, L. Binder, A modified activated carbon aerogel for high-energy storage in electric double layer capacitors, J. Power Source 163 (1) (2006) 616–622.
[50] Y. Nian, H. Teng, Nitric acid modification of activated carbon electrodes for improvement of electrochemical capacitance, J. Electrochem. Soc. 149 (8) (2002) A1008.